Ab initio study of step formation and self-diffusion on Ag(100)

Byung Deok Yu and Matthias Scheffler
Fritz-Haber-Institut der Max-Planck-Gesellschaft, Faradayweg 4-6, D-14195 Berlin-Dahlem, Germany
(Received 31 October 1996)

Using the plane-wave pseudopotential method, we performed density-functional theory calculations on the stability of steps and self-diffusion processes on Ag(100). Our calculated step formation energies show that the {111}-faceted step is more stable than the {110}-faceted step. In accordance with experimental observations we find that the equilibrium island shape should be octagonal very close to a square with predominately {111}-faceted steps. For the (100) surface of fcc metals atomic migration proceeds by hopping or exchange processes. For Ag(100), we find that adatoms diffuse across flat surfaces preferentially by hopping. Adatoms approaching the close-packed {111}-faceted step edges descend from the upper terrace to the lower level by an atomic exchange with an energy barrier almost identical to the diffusion barrier on flat surface regions. Thus, within our numerical accuracy ($\approx \pm 0.05$ eV), there is no additional step-edge barrier to descent. This provides a natural explanation for the experimental observations of the smooth two-dimensional growth in homoepitaxy of Ag(100). Inspection of experimental results of other fcc crystal surfaces indicates that our result holds quite generally. [S0163-1829(97)07319-0]

I. INTRODUCTION

The study of the morphology of surfaces is one of the oldest areas of crystal growth, and has attracted particular attention in recent years due to advances in epitaxy and the possibility of controlled growth of materials and bulk quality surfaces. The structure of an epitaxial film is often thought to be determined by thermodynamic principles, in which the film is assumed to adopt the energetically stable thermal-equilibrium structure.[1] However, there are many examples which demonstrate that, under typical growth conditions growth is often governed by kinetics rather than thermodynamics. A lot of experimental works show that the growth mode (the evolution of film structure with coverage) can be altered by varying growth conditions such as the substrate temperature and deposition rate, or by introducing defects or surfactants.[2] A notable example is the study of homoepitaxial growth of Ag(111): Under clean surface conditions the growing surfaces are very rough with mountains as high as 30–40 atomic layers (multilayer growth).[3,4] These studies revealed that the film structure is governed by the kinetics of surface diffusion. Hence, a knowledge of the kinetics such as mass transport across terraces and steps and the diffusion parallel to steps is essential to reach an understanding of the morphology and quality of growth.

To date, most calculations of atomic diffusion on surfaces employ computationally fast semiempirical methods. They have been widely used because of their methodological simplicity, and under the assumption that the results, although quantitatively not very accurate, may still explain general trends. The main approximation of these methods concerns the kinetic-energy operator of the electron and the neglect of a self-consistent adjustment of the electron density. Thus the essence of the mechanisms governing the breaking and making of chemical bonds is missing. Obviously, quite often, as e.g., in the example discussed in this paper, *quantitative* results determine the *qualitative* features. For example, when the energy barrier at the step edge is larger than the diffusion barrier at the flat surface, the growth mode is rough, and when the step-edge barrier is equal or smaller, the growth mode is flat. The proper treatment which gives quantitatively and qualitatively more accurate results, and takes the quantum-mechanical properties and the chemistry of interatomic interactions properly into account is density-functional theory (DFT).

In this paper we report DFT total-energy calculations of step formation and diffusion of Ag adatoms on the (100) surface of fcc silver, which extends work presented earlier.[5] Homoepitaxy of silver exhibits a different behavior in the growth mode, depending on substrate orientations: The growing surface of Ag(100) is smooth and flat, whereas that of Ag(111) is typically rather rough. For Ag(100) surfaces reflection high-energy electron-diffraction (RHEED) intensity oscillations have been observed[6] in the temperature range from 200 to 480 K, which indicates that the growth proceeds by a smooth two-dimensional (2D) mode. The same overall behavior was also obtained using helium scattering.[7] In contrast, for Ag(111) surfaces RHEED intensity oscillations are absent at all temperatures, suggesting that there is no 2D growth, but that the surface becomes very rough upon growth. This finding for Ag(111) was confirmed by x-ray reflection experiments[8] and scanning tunneling microscopy (STM) measurements.[3,4] The former study shows that the growth mode changes from multilayer to step-flow growth over the temperature range from 175 to 575 K. The latter studies show a STM topography of ''mountain and canyon''-like structures with heights of 30–40 atomic layers.

From their analysis of STM images for Ag(111), Vrijmoeth *et al.*[3] concluded that the multilayer growth is attributed to an additional step-edge barrier. This is the barrier for a diffusing adatom descending steps minus the surface diffusion barrier. The authors obtained that the additional energy barrier is 0.15 eV. Bromann *et al.*[4] developed a method to determine with high accuracy attempt frequencies and activation energies for terrace diffusion as well as for the step-down process. This analysis was done by measuring the

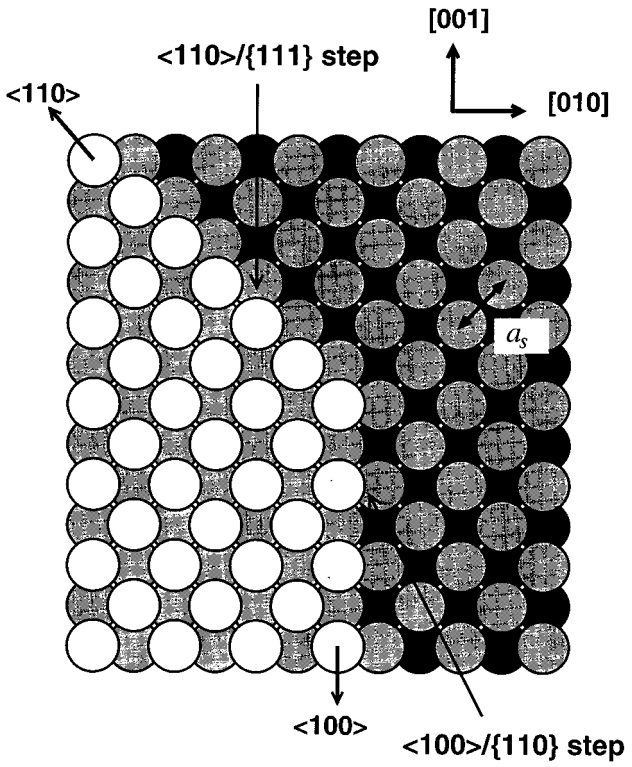

FIG. 1. Top view of monolayer-high terrace on a fcc (100) surface: a {111}-microfaceted step running along the ⟨110⟩ direction and a {110}-microfaceted step running along the ⟨100⟩ direction. The two step edges are labeled ⟨110⟩ / {111} and ⟨100⟩/ {110}, respectively. For our example Ag(100) the nearest-neighbor spacing, i.e., the surface lattice constant a_s, is 2.92 Å.

nucleation rate on top of islands as a function of island size and temperature. For the additional energy barrier they obtained a value of 0.12 eV, very close to the value of 0.15 eV obtained by Vrijmoeth *et al.* Recent STM studies by Morgenstern *et al.*[9] found the additional step-edge barrier to be 0.10 eV. This additional energy barrier, which adatoms encounter at step edges, explains why the growth of silver perpendicular to the (111) surface proceeds by a very rough multilayer mode. Interestingly, as noted above, the growth of the (100) surface is qualitatively different. As the calculations in Ref. 5 showed, the additional step-edge barrier is practically zero. Below, we extend our previous study and repeat convergence tests. Furthermore, we consider the shape of islands formed on Ag(100) in thermal equilibrium. There are two types of monolayer-high steps for fcc (100) surfaces as shown in Fig. 1: One is a close-packed step running along the ⟨110⟩ direction which has a {111} microfacet at the edge, and the other an open step running along the ⟨100⟩ direction which has a {110} microfacet at the edge. The ratio of formation energies of these two steps determines the equilibrium shape of islands on Ag(100) (as obtained by the Wulff construction).[10] Here we apply density-functional theory to evaluate the energies of these two sorts of steps.

The paper is organized as follows. In Sec. II, we describe the method of calculation. In Sec. III, the equilibrium shape of islands is discussed as it follows from our calculated step-formation energies. In Sec. IV we present results for diffusion processes of a Ag adatom on flat and stepped Ag(100) surfaces, and discuss their implication on epitaxial growth. Finally the paper is concluded in Sec. V.

II. METHOD OF CALCULATION

The total energies and forces on atoms are calculated by DFT. We use a norm-conserving pseudopotential method together with an iterative minimization of the Kohn-Sham total energy.[11] The electronic wave functions are expanded in a plane-wave basis set. Most calculations have been carried out using the local-density approximation (LDA) for the exchange-correlation functional.[12] At important geometries we repeated the calculations using the generalized gradient approximation (GGA) of Perdew *et al.*[13]

We use a repeating slab geometry to simulate the actual surface. A 3×3 periodicity is employed in the lateral directions, which when tested shows that artificial adatom-adatom interaction is sufficiently weak and in fact negligible for the questions of concern. An artificial periodicity is imposed along the perpendicular direction to the surface to construct a three-dimensional unit cell. We take a slab of three atomic layers and of a 10.35-Å vacuum region. This rather thin slab is acceptable, as we adsorb the adatom on only one side.[14] We relax the adatom and the top-layer atoms according to a damped Newton dynamics, while the other atoms in the two bottom layers are kept at the bulk positions. The optimized geometries are identified by the requirement that the remaining forces acting on the atoms are smaller than 0.05 eV/Å.

The LDA (GGA) ionic pseudopotentials are created using the nonrelativistic (semirelativistic) scheme of Troullier and Martins.[15] The fully separable norm-conserving pseudopotentials of Kleinman-Bylander form[16–18] are constructed with the *s* pseudopotential as the local component. The tightly bound $4d$-electron states are treated as valence states. We use a kinetic-energy cutoff of 40 Ry to expand the wave functions in plane waves. The **k**-space integration is performed using nine equidistant **k** points in the surface Brillouin zone (SBZ) of the 3×3 cell. To improve the **k**-space integration and stabilize convergence, the electronic states are occupied according to a Fermi distribution with $k_BT_{\rm el}=$ 0.1 eV,[14] and then the total energies are extrapolated to zero electronic temperature. In order to attain the iterative solutions of the Schrödinger equation, we start with initial wave functions obtained from the self-consistent solutions to the Kohn-Sham Hamiltonian in a mixed basis set of pseudoatomic orbitals and plane waves with a cutoff energy of 4 Ry, as developed by Kley *et al.*[19] This approach gives much faster convergence than the conventional one starting with the initial wave functions created from the diagonalization of the Hamiltonian and a small cutoff energy in the plane-wave basis set.

To test the accuracy of the pseudopotentials, we calculated the ground-state properties of bulk silver, using 512 **k** points in the Brillouin zone. The results derived from the Murnaghan equation-of-state fit to the calculated data are listed in Table I. Zero-point vibrations are not considered in these theoretical results. The calculated values are in good agreement with $T\rightarrow0$ K experimental data.

TABLE I. Structural properties of fcc silver obtained from the plane-wave pseudopotential and all-electron linearized-augmented-plane-wave (LAPW) methods, for nonrelativistic (NR) and semirelativistic (SR) calculations in the LDA and GGA. The $T \rightarrow 0$ K experimental data are given for comparison.

	This work		LAPW[a]		
	LDA (NR)	GGA (SR)	LDA (SR)	GGA (SR)	Expt.[b]
a_0 (Å)	4.14	4.18	4.00	4.17	4.07
B_0 (GPa)	99	90	136	85	102

[a]Reference 20.
[b]The experimental values are taken from Ref. 20.

III. STEP FORMATION ON (100) SURFACES

A. Structure and energetics of the flat surface

Before we describe the step formation on Ag(100), it is worthwhile to study the properties of the flat Ag(100) surface. The surface formation energy per surface atom is given as

$$\gamma = (E_{\text{slab}} - N_{\text{Ag}}\mu_{\text{Ag}})/N_{\text{surf}}, \tag{1}$$

where E_{slab} is the total energy of the slab of N_{Ag} silver atoms and N_{surf} is the number of atoms at the surfaces (e.g., for a 2×2 cell $N_{\text{surf}}=8$). In thermal equilibrium the silver chemical potential is equal to the energy of a silver atom in the bulk. In order to achieve an optimum of error cancellations the calculation of the bulk energy μ_{Ag} is done with the same **k**-point sampling as in the slab calculations. The work function is given by the difference between the electrostatic energy in the middle of the vacuum region and the Fermi energy. The multilayer relaxation Δd_{ij} is defined by the change in spacing between layers i and j compared to the interlayer spacing in the bulk, d_0.

We calculate the properties of flat Ag(100), using a slab of five atomic layers, a vacuum region equivalent to five atomic layers, and 96 **k** points in the SBZ of the 1×1 cell. In this calculation we used the lattice constant 4.14 Å from a **k**-sampling-converged calculation which differs only by 0.1% from the calculated lattice constant using the above **k** points. The results are summarized in Table II. The results in our previous paper[5] were obtained using a slab of four atomic layers, a vacuum region equivalent to four layers, and 64 **k** points in the SBZ of the 1×1 cell. Due to these changes the present results differ slightly from those of Ref. 5. The calculated results are in good agreement with a previous full-potential linear-muffin-tin-orbital (FP-LMTO) calculation.[21,22] Our calculations of the lattice relaxation give $\Delta d_{12}/d_0 = -2.2\%$ and $\Delta d_{23}/d_0 = 0.4\%$. The low-energy electron-diffraction analysis,[25] in which the first (d_{12}) and second (d_{23}) interlayer spacings were determined, shows small relaxations with $\Delta d_{12}/d_0 = 0 \pm 1.5\%$ and $\Delta d_{23}/d_0 = 0 \pm 1.5\%$. This result is in good agreement with the present DFT-LDA results within the experimental accuracy (see also the influence of surface vibrations, which is neglected in this calculation[26]).

TABLE II. Calculated results for the properties of flat Ag(100): surface formation energy γ, work function ϕ, and multilayer relaxation Δd_{ij} relative to the interlayer spacing in the bulk d_0. It is noted that the experimental surface energy is an estimate from liquid surface tension measurements.

	γ (eV/atom)	ϕ (eV)	$\Delta d_{12}/d_0$ (%)	$\Delta d_{23}/d_0$ (%)
This work (NR–LDA)	0.57	4.39	−2.2	0.4
FP-LMTO (NR–LDA)[a]	0.63	4.43	−1.9	
FP-LMTO (SR–LDA)[b]	0.62	4.77	−1.9	
Expt.	0.65[c]	4.64[d]	0 ± 1.5[e]	0 ± 1.5[e]

[a]Reference 21.
[b]Reference 22.
[c]Reference 23.
[d]Reference 24.
[e]Reference 25.

B. Structure and energetics of steps

In this subsection we consider the stability of the two most densely packed monolayer-high steps on Ag(100): the close-packed $\langle 110 \rangle / \{111\}$ and open $\langle 100 \rangle / \{110\}$ steps (see Fig. 1). To compute step energies we use the slab geometry of the grooved surface sketched in Fig. 2.

The simulation cell has the periodicity of L_x along the step edge and of L_y along the perpendicular direction to the step edge. We take L_x to be a_s and $\sqrt{2}a_s$ for {111}- and {110}-faceted steps, respectively. L_y is treated as a variable, so that the ledge separation l is equal to $L_y/2$ (see Fig. 2). The formation energy of the grooved surface E_{surf} is extracted from the calculations of the N-layer slab shown in Fig. 2, by applying the formula

$$E_{\text{surf}}(N) = E_{\text{slab}}(N) - N_{\text{Ag}}\mu_{\text{Ag}}. \tag{2}$$

The step formation energy per unit length is

$$\lambda(N) = [E_{\text{surf}}(N) - N_{\text{surf}}\gamma(N)]/L_x. \tag{3}$$

In Eq. (3), $\gamma(N)$ is the surface energy per surface atom from the calculations of the N-layer slab of the flat (100) surface, and N_{surf} is the number of surface atoms at the grooved surface: $N_{\text{surf}} = L_x L_y / a_s^2$. The surface energy is evaluated by averaging the surface energies of the thin and thick region of the slab, i.e., $\gamma_{\text{ave}}(N) = (1-\alpha)\gamma(N) + \alpha\gamma(N+1)$ (α is a ra-

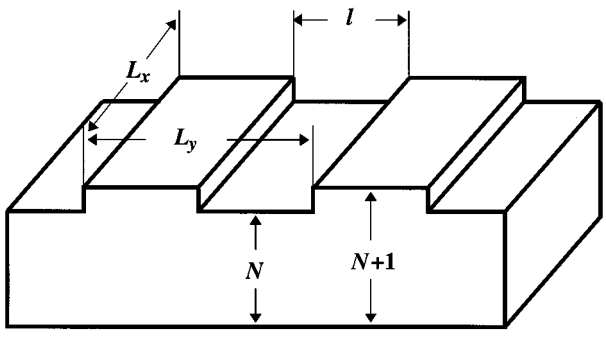

FIG. 2. Schematic representation of the N-layer slab of the grooved surface. Periodic boundary conditions are applied along the x and y axes.

TABLE III. Convergence of the formation energy of the {111}-faceted step in the relaxed geometry as a function of ledge separation l and the number of atomic layers N, calculated by DFT-LDA.

N	3	3	3	4
l (a_s)	2	3	4	3
E_{surf} (eV) [Eq. (2)]	4.951	7.258	9.593	7.172
γ_{ave} (eV/atom)	0.579	0.579	0.581	0.576
λ (eV/a_s) [Eq. (3)]	0.160	0.155	0.152	0.130

tio of the number of surface atoms in the thick region and the total number of surface atoms). The averaging improves the accuracy of the calculated step energies.

Several calculations were done to test the dependence of the calculated step energies on the ledge separation l and the number of atomic layers N. The results of the {111}-faceted step are summarized in Table III. It shows that the step energy decreases with increasing ledge separation l. In particular, the step energy λ can be expanded with respect to the ledge separation[27]

$$\lambda = \lambda_0 + A/l^2. \tag{4}$$

In this equation the first term is the energy of an isolated step, and the last term gives the effective interaction between steps. This term includes possible energetic contributions such as dipole-dipole or elastic interactions. For the three-layer grooved surface we obtain $\lambda_0 = 0.150$ eV/a_s and $A = 0.041$ eV/a_s^3 in the relaxed geometry by fitting the variation of the step energy with the ledge separation l to Eq. (4). We find that the step energy already reaches the isolated one at $l = 3a_s$ with an error of 0.005 eV/a_s. The step energy decreases by 0.024 eV/a_s or 20% when increasing the slab thickness from three to four layers, while the ratio of the step energies changes very slightly (only 5%). Thus, we see that a slab of four layers is sufficient to obtain reasonably converged result for the ratio of step energies.

Using the four-layer slab of the grooved surface and a ledge separation of $3a_s$, we obtain the formation energy of 0.130 eV/a_s (LDA) for the close-packed {111}-faceted step. For the {110}-faceted step we take a four-layer slab and a ledge separation of $2\sqrt{2}a_s$. The obtained step energy is 0.156 eV/a_s (LDA). Thus the close-packed {111}-faceted step is more stable than the open {110}-faceted one. This confirms the experimental observation that the {111}-faceted steps are preferentially formed in thermal equilibrium. This result is not unexpected because of atomic geometries, i.e., the local coordinations of the two steps differ noticeably: A step-edge atom at the {111}-faceted step has seven nearest neighbors, while a step-edge atom at the {110}-faceted step has only six neighbors. Using the AFW (Adams-Foiles-Wolfer[28]) EAM (embedded-atom method) functions, Nelson, Einstein, and Khare[29] found λ to be 0.102 and 0.142 eV/a_s for {111}- and {110}-faceted steps, respectively. With the VC (Voter-Chen[30]) functions they obtained λ to be 0.135 eV/a_s for {111}-faceted step.

When the formation energies of all steps are known, the equilibrium shape of an island can be obtained by finding the island shape with minimum free energy, or by applying the Wulff construction.[10] For the (100) surface it is certainly plausible that only two steps are important. Thus we expect octagonally shaped islands, as shown in Fig. 3. The calculated step formation energies imply that the {111}-faceted edges should dominate, and that the edge-length ratio should be $L^{\langle 100\rangle/\{110\}} : L^{\langle 110\rangle/\{111\}} = 3 : 10$. This theoretical finding can be compared to experimental observations. In fact, for an ion-bombarded Ag(100) surface the preferential formation of close-packed {111}-faceted step edges has been observed at room temperature,[31] and for Ir(100) Chen and Tsong, using the field ion microscope, also found that the equilibrium island shape is rectangular with {111}-faceted steps.[32]

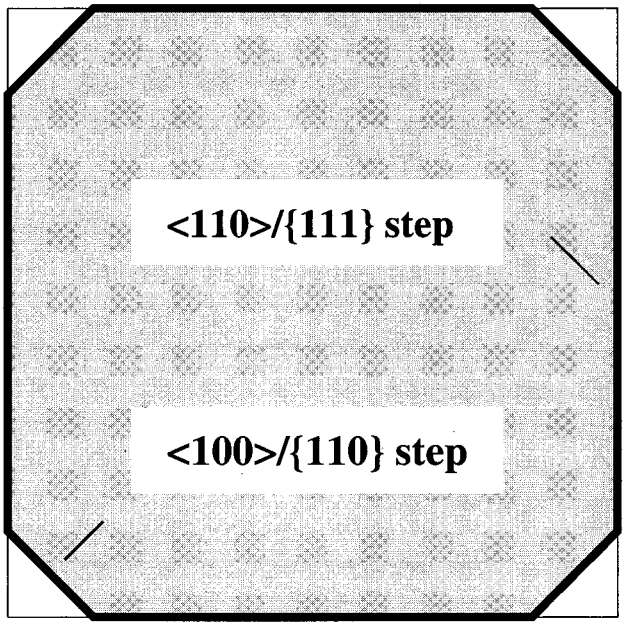

FIG. 3. Calculated shape of islands in thermal equilibrium. The close-packed {111}-faceted edges are longer than the open {110}-faceted ones. The edge length ratio is $L^{\langle 100\rangle/\{110\}} : L^{\langle 110\rangle/\{111\}} = 3{:}10$.

Next we consider the relaxations of the stepped surface. Figure 4 shows the geometry optimized structure of {111}-faceted steps. The relaxations of surface atoms in the upper terrace are nearly identical to those of surface atoms of flat Ag(100): surface atoms 1, 1′, and 1″ relax toward the bulk by $\sim$ 2 % of the bulk interlayer spacing d_0 [see Fig. 4(a)]. Atoms 2 and 2′ at step bottom slightly relax upward and toward atoms 3 and 3′, but these relaxations of lower terrace atoms are nearly negligible. Figure 4(b) displays the bond lengths of step-edge atoms with their underlying nearest neighbors, and the numbers show that the bond lengths are very close to those between surface atoms and their nearest neighbors in the subsurface sites of flat Ag(100). Similarly, at a grooved surface with {110}-faceted steps, downward relaxations of upper terrace atoms dominate.

IV. SELF-DIFFUSION ON FLAT AND STEPPED (100) SURFACES

A. Adsorption and self-diffusion on flat surfaces

We now present the results of adsorption and diffusion of a Ag adatom on the flat Ag(100) surface. For metals, metal adatoms on surfaces preferentially adsorb at the highest co-

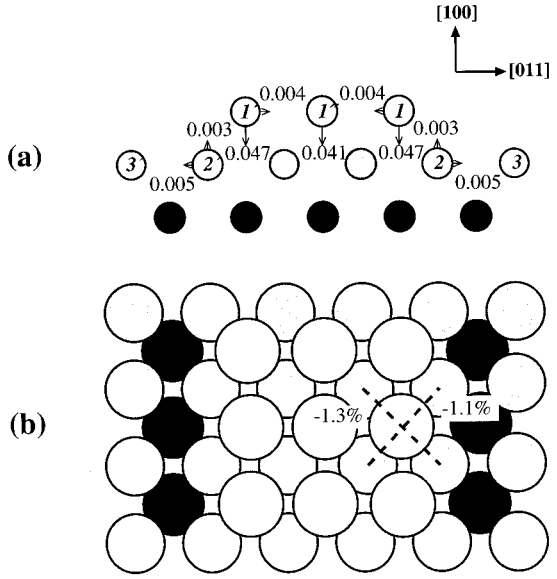

FIG. 4. (a) Side and (b) top views of the stable geometry of the grooved surface of the ledge separation $3a_s$ with {111}-faceted steps. In (a) arrows and numbers in unit of Å indicate directions and magnitudes of atomic displacements from the unrelaxed ideal step geometry. The percentage changes in distances to nearest neighbors of step-edge atoms relative to the nearest-neighbor separation in bulk are noted in (b).

ordination site. Indeed the equilibrium adsorption site for a Ag adatom on Ag(100) is the fourfold hollow [Fig. 5(a)]. In the optimized geometry, the four nearest neighbors of the adatom slightly distort in the lateral directions, opening the hollow site even further. The lateral displacement from the ideal clean surface site is 0.02 Å. The adatom is located 1.84 Å above the surface layer, and the bond length between the adatom and its neighbors is 2.78 Å, i.e., 5% shorter than the interatomic distance in the bulk. This follows the typical trend, namely, that bond strength per bond decreases with coordination and, correspondingly, bond length increases with coordination.

In metal-on-metal surface diffusion, an adatom typically moves across a flat surface by a series of hops between adjacent equilibrium adsorption sites. For fcc (100) an adatom in a fourfold site moves over the twofold bridge site into a neighboring fourfold hollow site [see Fig. 5(b)]. An adatom

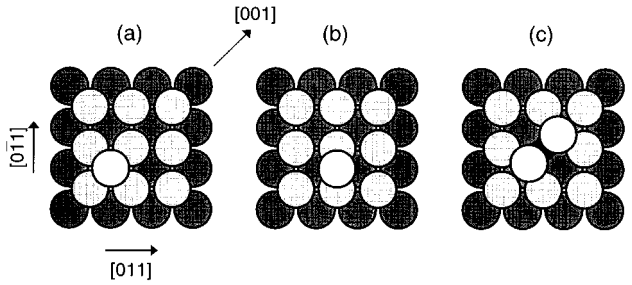

FIG. 5. Top view of an adatom at (a) the fourfold hollow site, (b) the transition state for the hopping diffusion (the twofold bridge site), and (c) the transition state for the exchange diffusion. The white and gray circles represent the adatoms and surface atoms, respectively.

may visit all the fourfold hollow sites, forming a 1×1 square pattern. An alternative mechanism for surface diffusion is atomic exchange where a diffusing atom moves by displacing a neighboring surface atom. For the fcc (100) surface the exchange process of an adatom with a surface atom occurs preferentially in the [010] and [001] directions. At the saddle point of the transition the adatom and surface atom are above a vacated surface-layer site [see Fig. 5(c)]. Subsequently the displaced surface atom becomes an adatom in a next-nearest-neighbor fourfold hollow site. When this diffusion mechanism is active, an adatom may visit only half of the fourfold hollow sites, forming a $c(2\times2)$ square pattern. Experimental evidences of the self-diffusion by exchange displacement on fcc (100) were obtained by Kellogg and Feibelman on Pt(100),[33] and by Chen and Tsong on Ir(100).[34] The process has been studied theoretically by Feibelman for Al(100).[35] His total-energy calculations of the self-diffusion barrier on Al(100) show that atomic diffusion via exchange is energetically favored by a factor of 3 over hopping. It is an open question if the exchange diffusion plays a role for other fcc(100) surfaces as well. The EAM calculations of Liu *et al.*[36] suggest that, besides Pt(100) and Ir(100), exchange displacements are also favored for self-diffusion on the (100) surfaces of Pd and Au. For self-diffusion on Cu(100), effective-medium calculations[37] predicted that exchange displacement occurs preferentially, but this result is in contrast to other semiempirical studies[36] and to a DFT-LDA calculation.[38]

Our total-energy calculations for the self-diffusion on Ag(100) clearly show that the hopping mechanism is energetically favored. The energy barriers for hopping diffusion are 0.52 eV (LDA) and 0.45 eV (GGA), which are close to the result of a FP-LMTO LDA calculation,[22] which obtained 0.50 eV. Using the AFW and VC EAM functions Liu *et al.*[36] obtained a similar value, namely, 0.48 eV. Our results show that the use of the GGA functional for the exchange-correlation energy lowers the energy barrier by 13% (0.07 eV) compared to the LDA result. Recent STM studies of homoepitaxy on Ag(100),[39] combined with Monte Carlo simulations using an appropriate model for fcc (100) homoepitaxy, determined the diffusion barrier to be 0.33 eV. Low-energy ion-scattering measurements of Langelaar, Breeman, and Boerma[40] obtained a value of 0.40 eV. At this point we note that the experimental analyses of the diffusion barriers are not without problems. Thus we conclude that our GGA result ($E_d=0.45$ eV) (Ref. 5) is in good agreement with (subsequently obtained) available experimental information. In the optimized geometry of the bridge site, the saddle point for the hopping diffusion, the two nearest neighbors of the adatom are pushed away and downwards by 0.05 Å. The adatom is located 2.33 Å above the surface layer. The bond length between the adatom and its two neighbors is 2.69 Å, i.e., 3% shorter than in the fourfold hollow. This again follows the well-known trend: Each of the two bonds at the bridge site is stronger than each of the four bonds at the hollow site.

To obtain the energy barrier for the exchange diffusion, we compute the total energy of the transition state shown in Fig. 5(c). We obtain energy barriers of 0.93 eV (LDA) and 0.73 eV (GGA) which are much higher than that for the hopping process. Thus we conclude that Ag adatoms diffuse

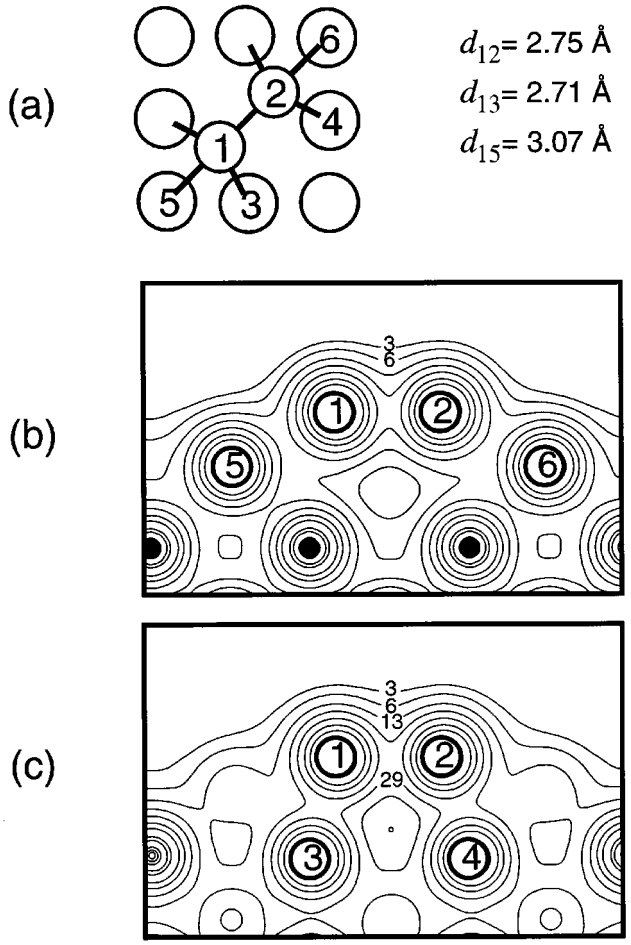

FIG. 6. Valence charge density at the transition state for the exchange diffusion. A schematic plot of the optimized atomic geometry is shown in (a). Panels (b) and (c) display the electron density. In (b) the plot is in the plane cutting atoms 5, 1, 2, and 6. In (c) the plot is in the plane cutting atoms 3, 1, 2, and 4. The value of the lowest-density contour is 3×10^{-3} e/(bohr)^3, and subsequent contours differ by a factor of 2.2. Solid circles mark the second-layer atoms.

across flat regions of Ag(100) by hopping. It is interesting that for the exchange geometry the difference between the LDA and GGA is noticeable (0.20 eV). The GGA value is comparable to the EAM results. Using the AFW and VC EAM functions, Liu *et al.* found energy barriers of 0.75 and 0.60 eV for the exchange process, respectively. In the optimized geometry of the transition state for the exchange diffusion [see Fig. 6(a)], each of the two topmost adatoms has four bonds with neighbors. The distance between the two topmost adatoms is 2.75 Å, 1% shorter than in the fourfold hollow. These two atoms are located 1.52 Å above the surface layer. The four atoms neighboring these atoms are pushed away by 0.06 Å and downwards by 0.05 Å. The bond length between the top-most and underlying Ag atoms is 2.71 Å, 3% shorter than in the fourfold hollow. Another bond length between the atoms 1 and 5 (between the atoms 2 and 6) in Fig. 6(a) is 3.07 Å, 10% longer than in the fourfold hollow, and 5% longer than in the bulk. We note that at the (100) surface of aluminum, the transition state of the exchange diffusion is supported by the formation of covalent

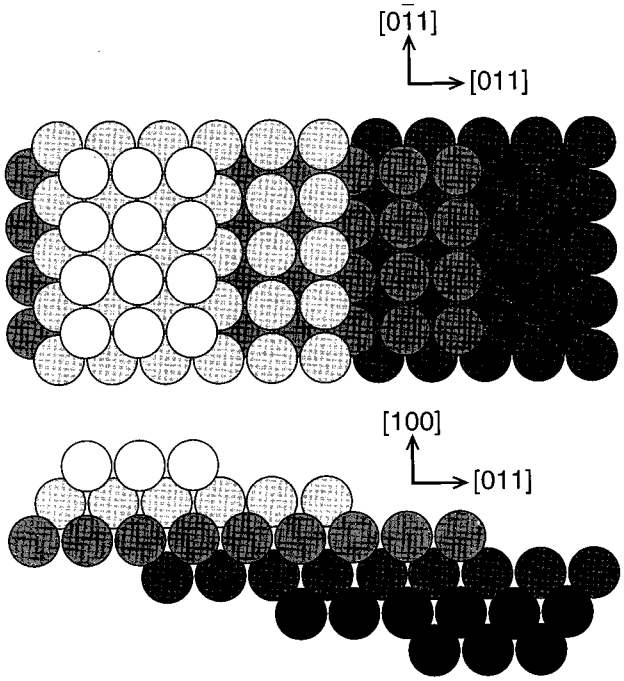

FIG. 7. Top and side views of the fcc (511) surface. The (511) surface has close-packed {111}-faceted steps and the number of atomic rows within the (100)-oriented terraces is three.

bonds, which is made possible (and indeed plausible) by the sp valence of the group-III element Al. For silver we find that the electron density does not reflect a pronounced covalency effect as shown in Figs. 6(b) and 6(c), which explains why the exchange displacement does not play a role at flat Ag(100).

B. Adsorption and self-diffusion on stepped surfaces

This section is concerned with the diffusion of a Ag adatom at the {111}-faceted steps which are preferentially formed on Ag(100) surfaces. The calculations were done for a high index (511) surface which is vicinal to (100) (see Fig. 7). This surface consists of (100) terraces which are three atom rows wide. The step edges are perpendicular to the [100] and [011] directions. The periodicity along the step edge is taken to be three surface lattice constants. Using a vicinal surface allows us to consider a smaller number of atoms within the unit cell than that required for the ordered step arrays on flat surfaces (the grooved surfaces). Using the vicinal (511) surface of four atomic layers, we obtain the formation energy of 0.136 eV/a_s (LDA) for the close-packed {111}-faceted step, which is close to the corresponding value 0.130 eV/a_s (LDA) from the four-layer slab calculations of grooved surface (see Table III). In Fig. 8(b) we display the total energy of a Ag adatom diffusing on the stepped Ag(100) by the hopping process. For any position of the path indicated in Fig. 8(a), the total energy is obtained by relaxing all coordinates of the atoms of the surface layer as well as the height of the diffusing atom.

Figure 8(b) clearly shows two stable adsorption sites: The hollow site (M) at the step, at which the adatom is fivefold coordinated, and the hollow site (H) on the terrace, at which the adatom coordination is four. Due to the higher coordina-

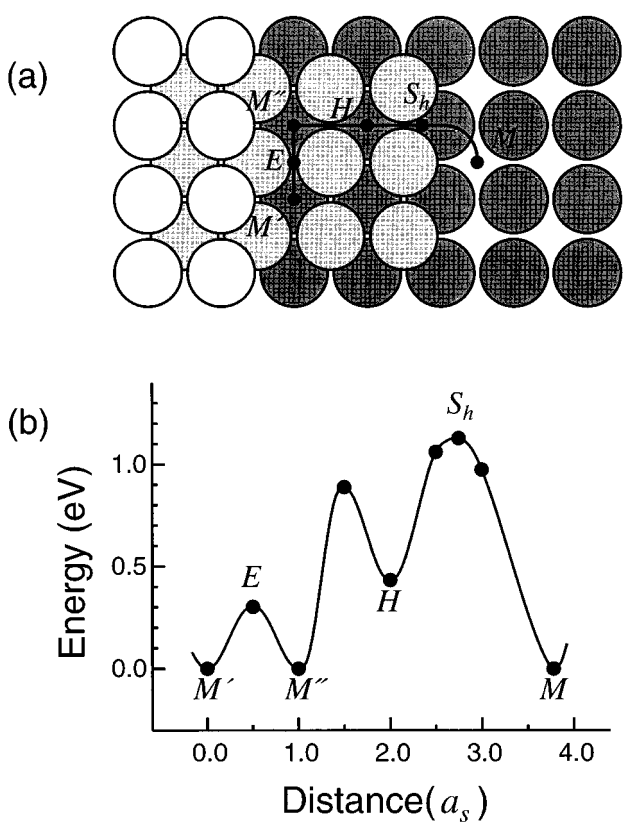

FIG. 8. Total energy of a Ag adatom diffusing along the indicated path by a hopping (rollover) process, calculated within the LDA. A top view of the vicinal (511) surface is shown in (a). The {111}-faceted edges are aligned along the [011] direction. The distance is given in unit of the surface lattice constant a_s.

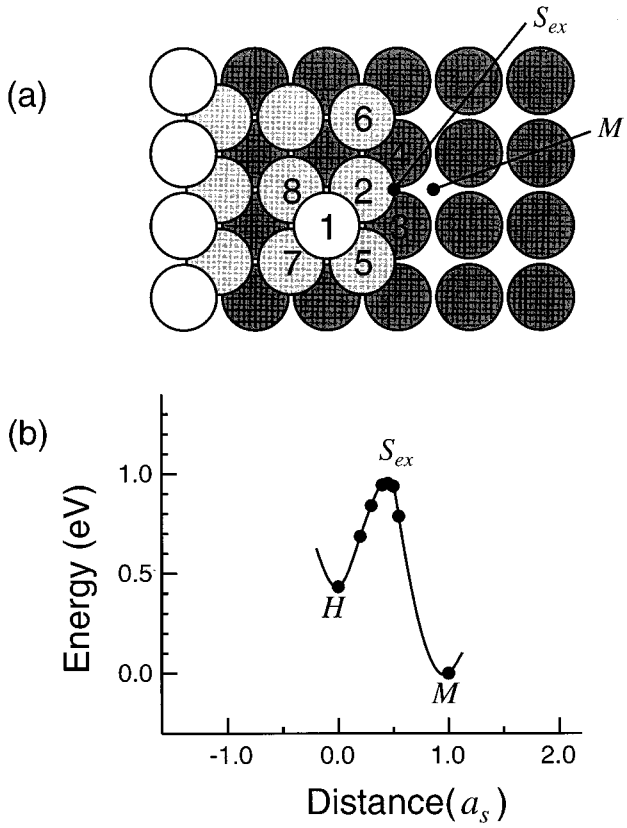

FIG. 9. Total energy of a Ag adatom diffusing across a step by an exchange process, calculated within the LDA. In (a), adatom 1 is adsorbed at the fourfold hollow site H. The total energy as a function of the distance of the step-edge atom 2 from the undistorted step edge is shown in (b).

tion it is indeed plausible that the DFT results give that the adsorption site M is more stable than site H. The energy differences between the M and H sites are 0.43 eV (LDA) and 0.32 eV (GGA). In the optimized geometry of the site M the distance between the step-edge atom and adatom is 2.89 Å, 1% shorter than in the bulk. The bond length between the two step-bottom atoms and adatom is 2.78 Å, and that between the two lower-terrace atoms and adatom is 2.84 Å. It is also interesting to note that desorption of an adatom at the step edge to the flat region requires to overcome a very high-energy barrier (LDA: 0.96 eV; GGA: 0.76 eV).

When the adatom rolls over the ledge from an H site on the upper terrace to an M site on the lower terrace, we obtain energy barriers of 0.70 eV (LDA) and 0.55 eV (GGA). Thus, we find the ''additional step-edge barriers'' to be 0.18 eV (LDA) and 0.10 eV (GGA), which step down from the upper terrace by the hopping (rollover) process. These values are higher by about 30% (20%) in the LDA (GGA) than the diffusion barrier at the flat region. At the transition state for the rollover process the adatom is located near the bridge site at the ledge [S_h in Fig. 8(a)]. In the optimized geometry the two nearest neighbors of the adatom are slightly pushed away, and the adatom is located 2.27 Å above the upper terrace. The bond length between the step-edge atoms and adatom is found to be 2.72 Å, 1% longer than in the bridge site at the flat region and 7% shorter than that of a bulk atom: Each of the two bonds at site S_h is weaker than that at the bridge site on the flat region. At the bridge site on the flat terraces the adatom has four next-nearest neighbors, while at S_h the adatom has two next-nearest neighbors. Thus we understand the additional energy barrier in terms of weaker bonds between the adatom and underlying surface atoms, and decrease of the number of the next-nearest neighbors compared to the flat surfaces.

The other possibility to step down from the upper terrace is via an exchange, where atom 2 moves toward the M site and atom 1 follows in close contact [see Fig. 9(a)]. Figure 9(b) displays the results of the step-down diffusion by the exchange process. Within our numerical accuracy for energy differences ($\approx \pm 0.05$ eV) the calculated energy barriers of 0.52 eV (LDA) and 0.45 eV (GGA) are almost identical to that of the hopping diffusion at the flat region. The transition state for the exchange process is identified to be near the bridge site formed by two step-bottom atoms 3 and 4 on the lower terrace [S_{ex} in Fig. 9(a)]. The geometry of the optimized structure of the transition state is given in Fig. 10. The topmost adatom (No. 1) is located 1.26 Å above the upper-terrace atoms. The height is much lower than the value of 1.52 Å at the flat region. Inspection of the geometry at S_{ex} shows that the local coordination of atoms 1 and 2 remains high: At S_{ex} each of the two atoms 1 and 2 has five bonds with neighbors, while at the saddle point of the exchange

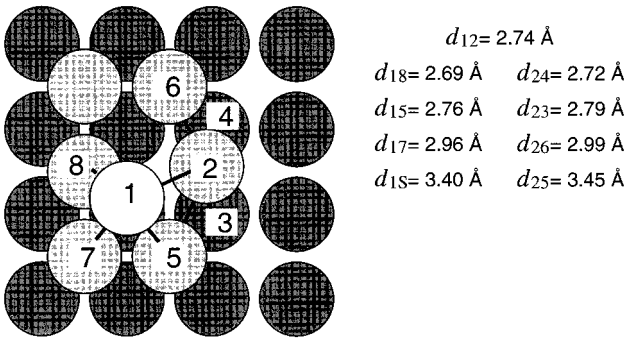

FIG. 10. Schematic view of the optimized atomic structure at the transition state S_{ex} of the step-down diffusion by the exchange process, calculated within the LDA. d_{1S} denotes the bond length between the adatom 1 and second-layer atom below.

diffusion on the flat region each of the two topmost atoms has only four bonds [Fig. 5(c)]. The origin of the lower diffusion barrier of the step-down motion by the exchange displacement compared to the flat region is thus the additional bonds formed at the obtained saddle point. Our finding that *there is no additional energy barrier to descend from the upper to the lower terrace* provides a natural explanation for the smooth 2D growth of silver at the (100) surface. By analyzing the STM images of Ag(100) during deposition, Zhang *et al.*[39] gave an estimate of 0.025 ± 0.005 eV for the additional step-edge barrier. Within our numerical accuracy ($\approx \pm 0.05$ eV) this is in good agreement with our result that the additional step-edge barrier is negligible.

Our finding that for Ag(100) an adatom goes down at step edges by an exchange process is expected to apply for other noble metals and other fcc transition metals as well. In fact, for homoepitaxial growth of Cu(100),[41] Pd(100),[42] and Ni(100),[43] damped oscillations of the scattering intensity have been observed. In order to explain the intensity oscillations associated with smooth 2D layer-by-layer growth, the step-edge barrier for the descent of adatoms was assumed to be negligible. For a hopping (rollover) process we expect that an adatom generally encounters an additional (positive) step-edge barrier [≈ 0.1 eV for Ag(100)] because of the low coordination of the transition state. Thus we expect that quite generally for fcc (100) metal surfaces step-down motion proceeds by an exchange process, similarly to Ag(100).

Finally we address the atomic motion along the close-packed {111}-faceted step to obtain ideas about the possible roughness of steps and kinetic growth shapes of islands. We find that the diffusion along the step edge proceeds by a hopping process. An adatom in a fivefold-coordinated adsorption site moves over a bridge site E into a neighboring fivefold-coordinated site [see Fig 8(a)]. From Fig. 8(b) we see that the barrier (LDA: 0.30 eV; GGA: 0.27 eV) is significantly lower than the surface diffusion barrier E_d (LDA: 0.52 eV; GGA: 0.45 eV). This lower energy barrier indicates that Ag islands formed on Ag(100) should be compact. Atoms which reach the step edges will certainly be able to diffuse parallel to the steps, and thus local thermal equilibrium is attained. We therefore expect rather straight step edges and no fractally shaped islands. In the optimized geometry of site E the distance between the two step-edge atoms and the adatom is 2.99 Å, 2% longer than in the bulk. We find the bond lengths of 2.66 Å between the step-bottom atom and adatom, and of 2.84 Å between the lower terrace atom and adatom, and note that the coordination varies from five to four as the adatom moves from site M' to site E [Fig. 8(a)], while for diffusion on flat terraces the coordination varies from four to two. Thus the lower barrier for diffusion parallel to steps can be understood in terms of the smaller variation in coordination.

V. CONCLUSION

In the above sections, we presented results of first-principles total-energy calculations for the electronic structure and energies of steps and for various microscopic self-diffusion processes at Ag(100). For fcc (100) surfaces, two types of monolayer-high steps are of particular importance: the close-packed {111}- and more open {110}-faceted steps. Our total-energy calculations show that the {111}-faceted step has a lower formation energy than the {110}-faceted one. This is understood in terms of different coordination of step-edge atoms. In accordance with experimental observations, we find that in thermal equilibrium the shape of an island should be octagonal, but very close to a square with {111}-faceted edges. The edge-length ratio of the octagon is calculated as 10:3. The energy barrier for self-diffusion of a Ag adatom along {111}-faceted edges is found to be significantly lower than the surface diffusion barrier. Thus we expect rather straight step edges and no fractally shaped islands.

At flat regions of Ag(100), Ag adatoms are found to diffuse by a hopping process. The obtained energy barrier is 0.45 eV in the GGA, which is very close to the experimental estimates, which are 0.40 eV (Ref. 40) and 0.33 eV.[39] In contrast to atomic motion on the flat region, the descent of adatoms at steps proceeds by an exchange process. The calculated energy barrier is almost identical to the barrier at the flat region. This indicates that there is no additional step-edge barrier to diffuse across step edges. This finding is in sharp contrast to the additional energy barriers [$\Delta E_{\text{step}}^{\text{Ag(111)}} = 0.15$,[3] 0.12,[4] and 0.107 eV (Ref. 9)] found experimentally at Ag(111), actuating a rough growth morphology. The calculated result implies good interlayer mass transport at Ag(100), and thus explains the smooth 2D growth experimentally observed in homoepitaxy of Ag(100). Inspection of details of the mechanism suggests that the step-down motion at steps by an atomic exchange process takes place quite generally for fcc (100) surfaces.

ACKNOWLEDGMENTS

We thank A. Kley, S. Narashimhan, G. Boisvert, C. Ratsch, and P. Ruggerone for helpful discussions. Enlightening discussions with G. Rosenfeld on various growth and self-diffusion experiments are gratefully acknowledged. B.D.Y. gratefully acknowledges the financial support from the Alexander von Humboldt Foundation.

[1] E. Bauer, Z. Kristallogr. **110**, 372 (1958).
[2] M. Scheffler, V. Fiorentini, and S. Oppo, in *Surface Science, Principles and Current Applications*, edited by R. MacDonald, E. Taglauer, and K. Wandelt (Springer, Berlin, 1996), p. 219; P. Ruggerone, Ch. Ratsch, and M. Scheffler, in *The Chemical Physics of Solid Surfaces*, Vol. 8, *Growth and Properties of Ultrathin Epitaxial Layers*, edited by D. P. Woodruff (Elsevier, Amsterdam, in press).
[3] J. Vrijmoeth, H. A. van der Vegt, J. A. Meyer, E. Vlieg, and R. J. Behm, Phys. Rev. Lett. **72**, 3843 (1994).
[4] K. Bromann, H. Brune, H. Röder, and K. Kern, Phys. Rev. Lett. **75**, 677 (1995).
[5] B. D. Yu and M. Scheffler, Phys. Rev. Lett. **77**, 1095 (1996).
[6] Y. Suzuki, H. Kikuchi, and N. Koshizuka, Jpn. J. Appl. Phys. **27**, L1175 (1988).
[7] P. Bedrossian, B. Poelsema, G. Rosenfeld, L. C. Jorritsma, N. N. Lipkin, and G. Comsa, Surf. Sci. **334**, 1 (1995).
[8] H. A. van der Vegt, H. M. van Pinxteren, M. Lohmeier, E. Vlieg, and J. M. C. Thornton, Phys. Rev. Lett. **68**, 3335 (1992).
[9] K. Morgenstern *et al.* (private communication).
[10] A. Zangwill, *Physics at Surfaces* (Cambridge University Press, Cambridge, 1988), p. 13.
[11] R. Stumpf and M. Scheffler, Comput. Phys. Commun. **79**, 447 (1994).
[12] D. M. Ceperley and B. J. Alder, Phys. Rev. Lett. **45**, 566 (1980); J. P. Perdew and A. Zunger, Phys. Rev. B **23**, 5048 (1984).
[13] J. P. Perdew *et al.*, Phys. Rev. B **46**, 6671 (1992).
[14] J. Neugebauer and M. Scheffler, Phys. Rev. B **46**, 16 067 (1992).
[15] N. Troullier and J. L. Martins, Solid State Commun. **74**, 613 (1990); Phys. Rev. B **43**, 1993 (1991).
[16] L. Kleinman and D. M. Bylander, Phys. Rev. Lett. **48**, 1425 (1982).
[17] X. Gonze, R. Stumpf, and M. Scheffler, Phys. Rev. B **44**, 8503 (1991).
[18] M. Fuchs *et al.* (unpublished).
[19] A. Kley *et al.* (unpublished).
[20] A. Khein, D. J. Singh, and C. J. Umrigar, Phys. Rev. B **51**, 4105 (1995).
[21] M. Methfessel, D. Hennig, and M. Scheffler, Phys. Rev. B **46**, 4816 (1992).
[22] G. Boisvert, L. J. Lewis, M. J. Puska, and R. M. Nieminen, Phys. Rev. B **52**, 9078 (1995).
[23] W. R. Tyson and W. A. Miller, Surf. Sci. **62**, 267 (1977); F. R. De Boer, R. Boom, W. C. M. Mattens, A. R. Miedema, and A. K. Niessen, *Cohesion in Metals* (North-Holland, Amsterdam, 1988).
[24] *Handbook of Chemistry and Physics*, 70th ed., edited by R. C. Weast (CRC Press, Boca Raton, FL, 1989).
[25] H. Li, J. Quinn, Y. S. Li, D. Tian, F. Jona, and P. M. Marcus, Phys. Rev. B **43**, 7305 (1991).
[26] J.-H. Cho and M. Scheffler, Phys. Rev. Lett. **78**, 1299 (1997).
[27] See, for instance, S. Kodiyalam, K. E. Khor, N. C. Bartelt, E. D. Williams, and S. Das Sarma, Phys. Rev. B **51**, 5200 (1995).
[28] J. B. Adams, S. M. Foiles, and W. G. Wolfer, J. Mater. Res. **4**, 102 (1989).
[29] R. C. Nelson, T. L. Einstein, and S. V. Khare, Surf. Sci. **295**, 462 (1993).
[30] A. F. Voter and S. P. Chen, in *Characterization of Defects in Material*, edited by R. W. Siegel, J. R. Weertman, and R. Sinclair, MRS Symposia Proceedings No. 82 (Materials Research Society, Pittsburgh, 1987), p. 375.
[31] Ch. Teichert, Ch. Ammer, and M. Klaua, Phys. Status Solidi A **146**, 223 (1994).
[32] C. Chen and T. T. Tsong, Surf. Sci. **336**, L735 (1995).
[33] G. L. Kellogg and P. Feibelman, Phys. Rev. Lett. **64**, 3143 (1990).
[34] C. L. Chen and T. T. Tsong, Phys. Rev. Lett. **64**, 3147 (1990).
[35] P. J. Feibelman, Phys. Rev. Lett. **65**, 729 (1990).
[36] C. L. Liu, J. M. Cohen, J. B. Adams, and A. F. Voter, Surf. Sci. **253**, 334 (1991).
[37] L. Hansen, P. Stoltze, K. W. Jacobsen, and J. K. Nørskov, Phys. Rev. B **44**, 6523 (1991).
[38] C. Lee, G. T. Barkema, M. Breeman, A. Pasquarello, and R. Car, Surf. Sci. Lett. **306**, L575 (1994).
[39] C.-M. Zhang, M. C. Bartelt, J.-M. Wen, C. J. Jenks, J. W. Evans, and P. A. Thiel, J. Cryst. Growth (to be published).
[40] M. H. Langelaar, M. Breeman, and D. O. Boerma, Surf. Sci. **352-354**, 597 (1996).
[41] H.-J. Ernst, F. Fabre, and J. Lapujoulade, Surf. Sci. Lett. **275**, L682 (1992).
[42] D. K. Flynn-Sanders, J. W. Evans, and P. A. Thiel, Surf. Sci. **289**, 75 (1993).
[43] S. T. Purcell, B. Heinrich, and A. S. Arrott, Phys. Rev. B **35**, 6458 (1987).